We are IntechOpen, the world's leading publisher of Open Access books Built by scientists, for scientists

4,800
Open access books available

122,000
International authors and editors

135M
Downloads

Our authors are among the

154
Countries delivered to

TOP 1%
most cited scientists

12.2%
Contributors from top 500 universities

WEB OF SCIENCE™

Selection of our books indexed in the Book Citation Index in Web of Science™ Core Collection (BKCI)

Interested in publishing with us?
Contact book.department@intechopen.com

Numbers displayed above are based on latest data collected.
For more information visit www.intechopen.com

Chapter 1

Production of Carbon Nanotubes and Carbon Nanoclusters by the JxB Arc-Jet Discharge Method

Tetsu Mieno and Naoki Matsumoto

Additional information is available at the end of the chapter

http://dx.doi.org/10.5772/51964

1. Introduction

Since the discovery of methods for the mass production of single-walled carbon nanotubes (SWNTs) [1, 2], applications of SWNTs such as transistor devices, biosensing devices, double-layer-type capacitors, transparent electrode films, radio wave absorbents and material hardeners have been studied [3-5]. Large-scale production and improvement of purity of SWNTs by the electric-arc techniques have been developed [6, 7]. However, the efficient production of high-quality and defect-free SWNTs, and metal/semiconductor selected or diameter-controlled production of SWNTs have not yet been achieved. Therefore, basic study of the various methods of producing SWNTs is still important, by which new high-performance routes to producing desired SWNTs are expected to be found.

Here, the production of SWNTs and carbon nanoclusters by the arc discharge method utilizing a magnetic field, known as the *JxB* arc-jet discharge method, has been studied [8-10]. Although the application of a steady-state magnetic field to arc discharge is not such a popular method, electromagnetic force can change the flow of hot gas in the arc region and thus control the production process of carbon clusters. To realize the large-scale production of carbon clusters by the arc discharge method, a revolver-injection-type *JxB* arc-jet producer was successfully developed by our group, by which the continuous mass production of SWNTs and other carbon clusters can be carried out.

As a result, the more efficient production of SWNTs and other carbon clusters compared with conventional arc discharge methods has been achieved. Here, the development of the *JxB* arc-jet discharge method and results obtained using the method are described.

2. Theoretical model of the *JxB* arc jet discharge method

By applying a steady-state weak magnetic field (B_0 = 1 – 5 mT) perpendicular to the discharge current in the arc discharge, the Lorentz force (*JxB* force) causes the ejection of the arc plasma and surrounding gas in the *JxB* direction as shown in Fig. 1 [8, 11]. In the 1960s, this force in a pulsed discharge was actively studied in relation to the electric propulsion engine of rockets [12].

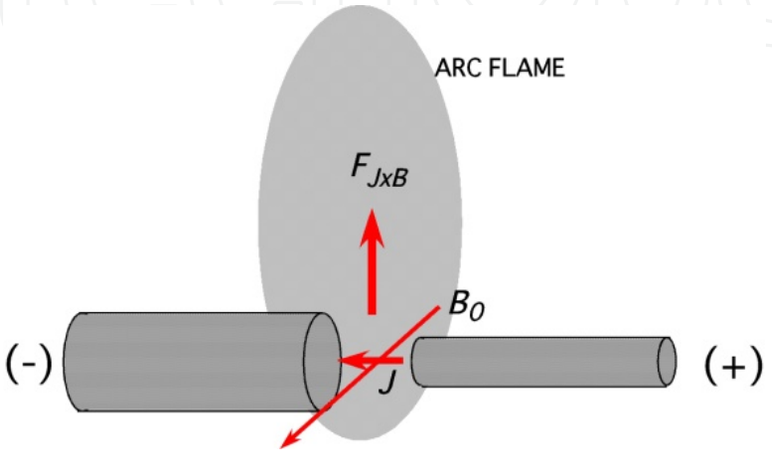

Figure 1. Schematic diagram of the *JxB* arc-jet discharge.

Here, this effect is used to eject sublimated carbon atoms in a selected direction. By controlling the magnetic field, control of the hot gas including the carbon material is possible, and suitable conditions to do hot gas reactions for the production of SWNTs and other carbon clusters can be selected. This method can also reduce the influence of the electrode direction and chamber configuration.

When the discharge current density and applied magnetic field are 50 A/cm^2 and 5 mT, respectively, the Lorentz force causing acceleration of electrons and ions is 0.25 N/cm^3. When the gas pressure and the gas temperature around the arc are 30 kPa and 5000 K, respectively, the mean free path and collision frequency of electrons are about 0.01 mm and 10 GHz, respectively. Because of this high collision frequency, electrons frequently collide with neutral gas atoms and accelerate them in the *JxB* direction, resulting in the ejection of hot gas from the arc region. The acceleration time is related to the electron lifetime in the plasma.

3. Production of carbon clusters by the *JxB* arc-jet discharge method

3.1. Heat flux

To investigate the *JxB* arc-jet discharge reaction, several types of arc reactors are used. Figure 2 shows a schematic of the reactor used to measure the heat flux of the arc plasma [11]. The reactor is made of stainless steel (18 cm diameter, 20 cm height) and has a carbon anode

http://dx.doi.org/10.5772/51964

(8.0 mm), a carbon cathode (15 mm), a viewing port and a movable calorimetric probe. The reactor is evacuated by a rotary pump to a pressure of less than 10 Pa and then closed. After introducing He gas with p(He) = 10 – 80 kPa, discharge starts, where the discharge current is I_d= 20 – 80 A and voltage between the electrodes is V_{rod}= 20 - 35 V. At the front and back of the reactor, solenoid coils (20 cm inner diameter) are installed to produce a steady state magnetic field of B_0= 0 - 5 mT.

When a magnetic field is applied during the discharge, the shape of the arc flame dramatically changes, and a strong plasma flow in the *J*x*B* direction can be observed. Figures 3(a) and (b) respectively show side views of the arc flames for B_0= 0 and B_0= 2.0 mT, where p(He)= 40 kPa and I_d= 80 A. The upper direction is the *J*x*B* direction. By applying a magnetic field, the plasma and the hot gas are ejected in the vertically upward direction. The upward flow of carbon particles can sometimes be clearly observed. By developing a calorimeter [11] in which flowing water absorbs the heat flux, the local heat flux is measured and the results are shown in Figs. 4 (a) and (b) [11]. By increasing the magnetic field, the heat flux is localized in the upper part of the arc plasma (FWHM value of about 50 mm). Above the arc plasma, the heat flux monotonically increases.

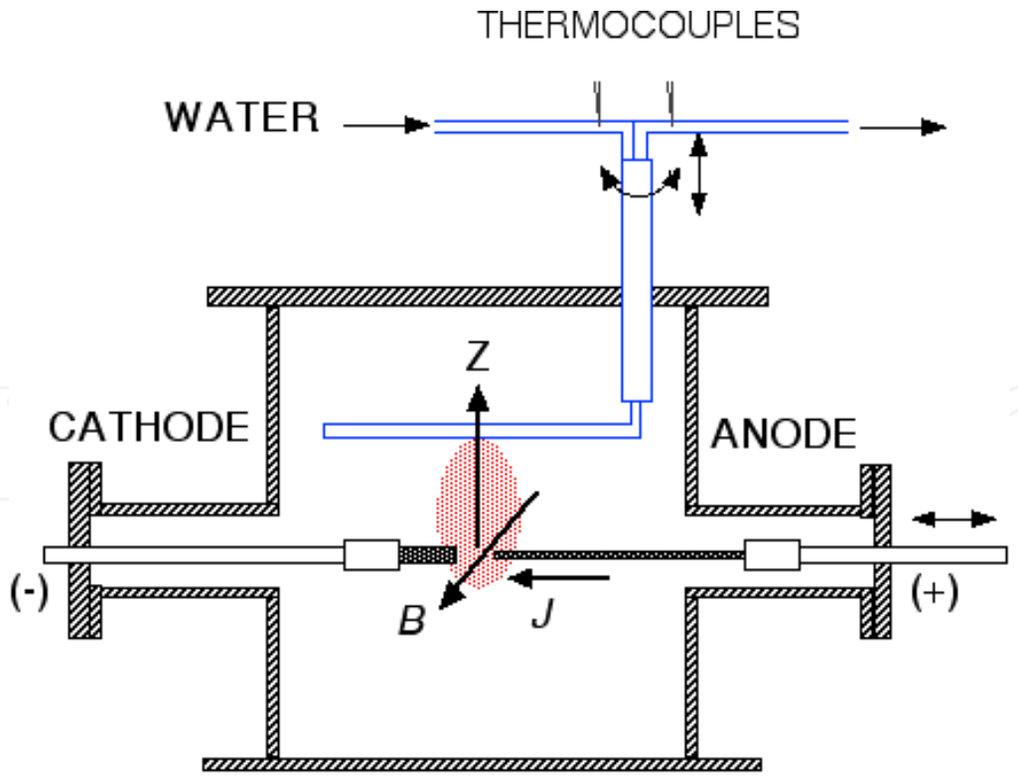

Figure 2. Schematic side view of the arc reactor with a calorimetric probe installed.

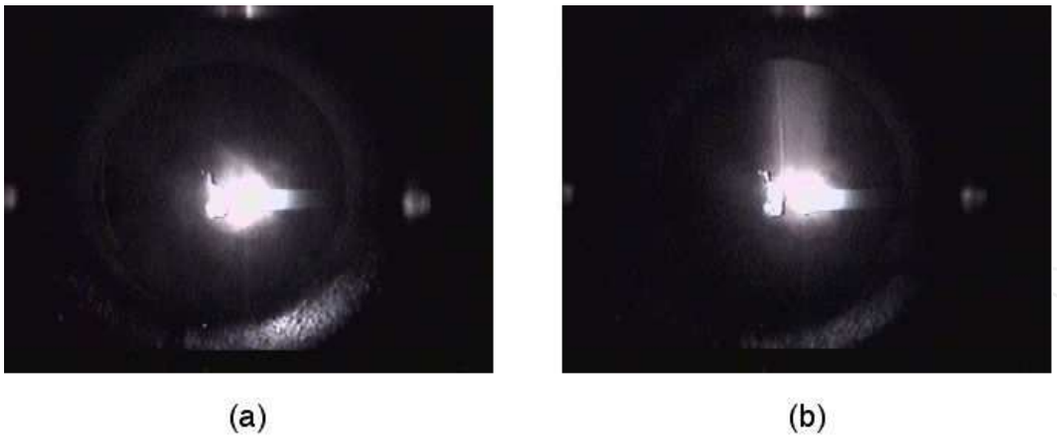

Figure 3. Arc flames for B_0= 0 (a) and B_0= 2.0 mT (b) (side views), where p(He)= 40 kPa and I_d= 80 A.

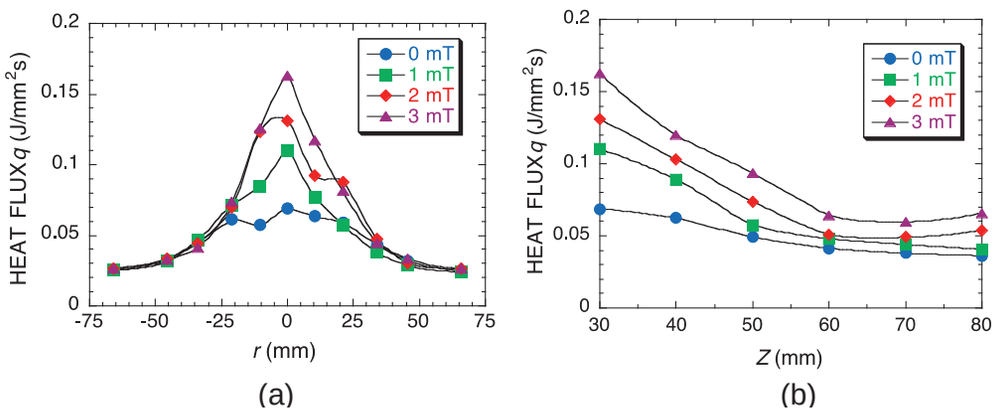

Figure 4. Radial profiles (a) and vertical profiles (b) of heat flux above the arc plasma for B_0= 0, 1.0, 2.0 and 3.0 mT. p(He)= 40 kPa and I_d= 60 A.

The heat flux above the arc plasma as a function of He gas pressure is measured and shown in Fig. 5(a), where I_d= 60 A, d_G= 5 mm, and the distance from the arc center is 40 mm. The heat flux increases monotonically with the pressure, which is particularly in the case of B_0= 2.0 mT. Figure 5(b) shows the heat flux above the arc plasma as a function of the gap distance between the two electrodes d_G, where p= 40 kPa, I_d= 60 A and z= 40 mm. By changing d_G, the effect of the arc jet changes, which can be observed from the viewing port. The heat flux gradually increases with the gap distance, and this effect is greatly enhanced when B_0= 2.0 mT.

To summarize these results, that the JxB arc jet is enhanced by increasing the applied magnetic field (B_0= 0 - 3.0 mT), the He pressure and the gap distance. However, under a stronger magnetic field of B_0> 4 mT, the discharge tends to be extinguished easily by fluctuation in the discharge.

http://dx.doi.org/10.5772/51964

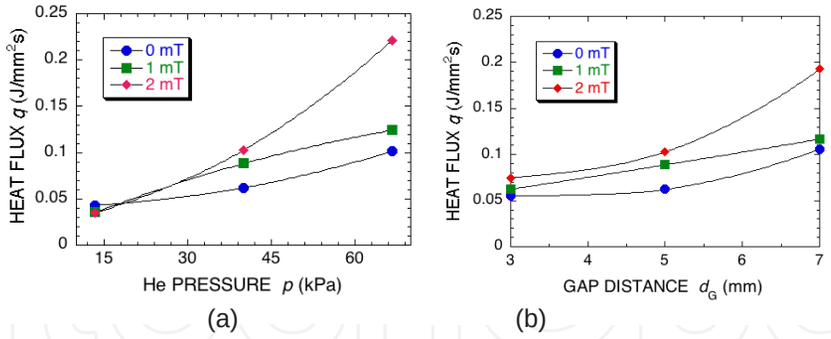

Figure 5. (a) He pressure dependence of the heat flux, where I_d= 60 A, d_G= 5 mm and z= 40 mm from the arc center. (b) Gap distance dependence of the heat flux, where p= 40 kPa, I_d= 60 A and z= 40 mm.

3.2. Relations among directions of the discharge current, magnetic field and gravity

In the case of gas arc discharge, gravity induces strong heat convection. Therefore, by changing the current direction relative to that of gravity, different production characteristics of carbon can be expected [13]. Direction of the ***JxB*** force compared with that of gravity should also be an important parameter. To examine the relations among the directions of the discharge current, magnetic field and gravity for the production of fullerenes, five experimental configurations are prepared and a discharge experiment is carried out. The 5 configurations are shown in Fig. 6. Here, the carbon anode is 6.5 mm in diameter and the carbon cathode is 15 mm in diameter.

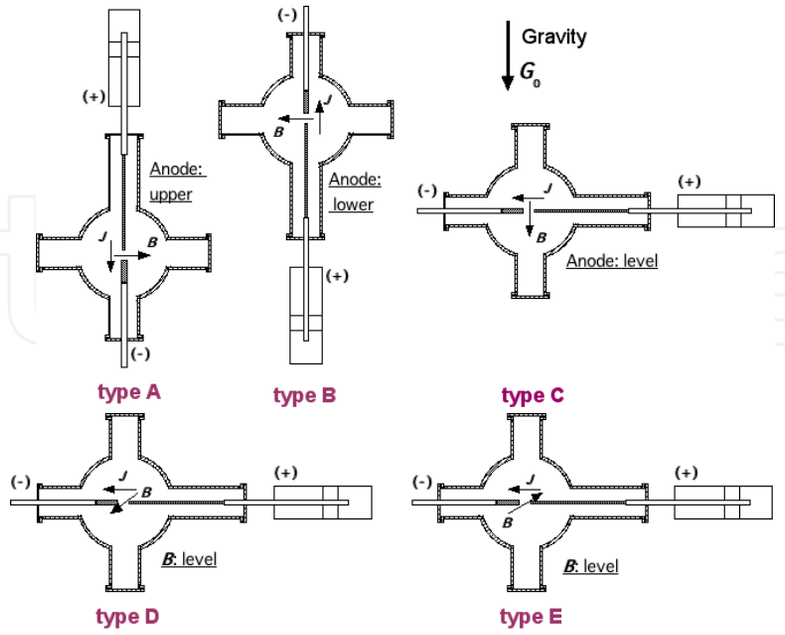

Figure 6. Schematic of five experimental configurations. The directions of the discharge current J and magnetic field B relative to that of gravity G_0 are changed.

The production rates of carbon soot W_{soot} (g/h) as a function of B_0 for configurations (types A – E) are obtained and the results are shown in Fig. 7, where p(He) = 40 kPa, I_d= 70 A and d_G~ 5 mm [13]. Generally, the soot production rate increases steadily with the magnetic field. However, for type A, W_{soot} is very low for B_0 =0 and it rapidly increases with increasing magnetic field. When B_0= 4.0 mT, the differences in W_{soot} are very small among the five configurations.

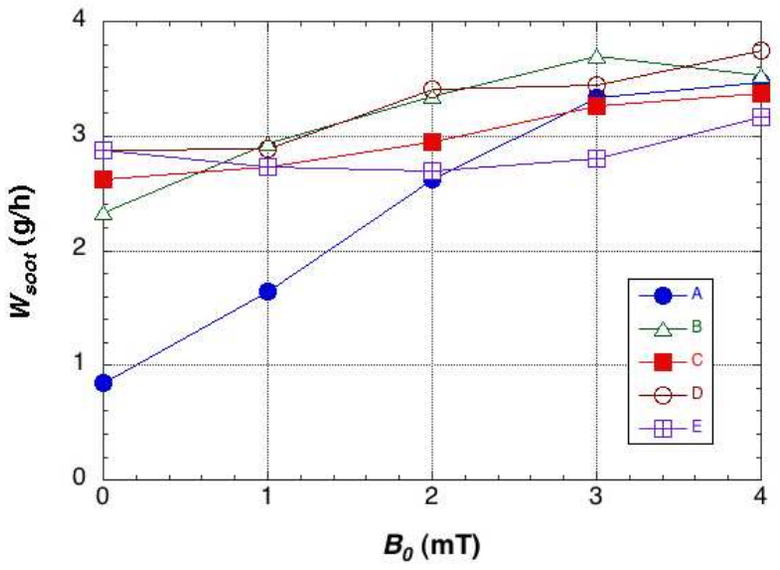

Figure 7. Production rate of carbon soot versus B_0 for the five configurations. p= 40 kPa, I_d= 70 A and discharge time T_d= 60 min

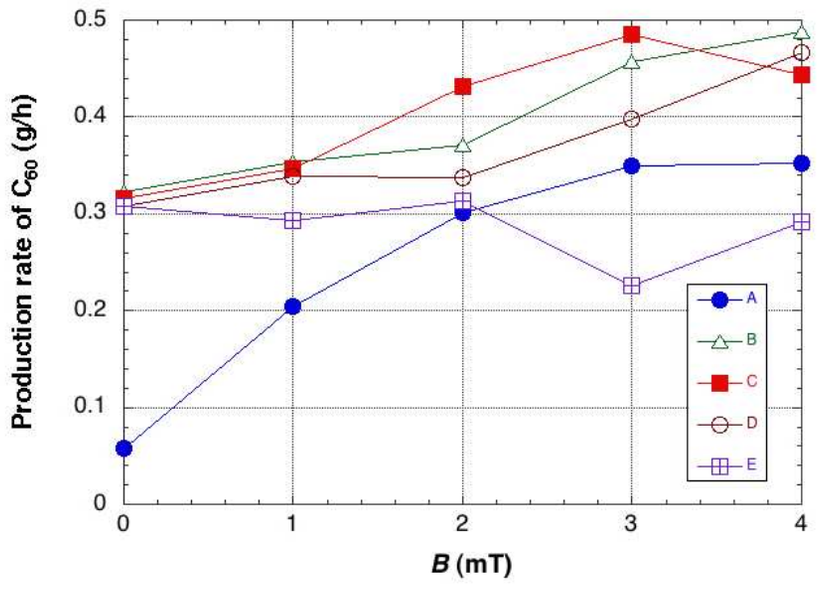

Figure 8. Production rate of C_{60} versus B_0 for the five configurations. p= 40 kPa, I_d= 70 A and discharge time T_d= 60 min.

The production rate of C_{60} as a function of B_0 for configurations (types A – E) is obtained and the results are shown in Fig. 8, where the conditions are the same us those of Fig. 7. Similarly to in Fig. 7, the C_{60} production rate generally increases with B_0, except for type A. C_{60} production rate of type A is very low at $B_0 = 0$. Moreover, for type E, the C_{60} production rate does not increase monotonically with B_0 and the magnetic field does not have a positive effect on the production rate.

From these results, it can be concluded that the directions of the discharge current and magnetic field compared with that of gravity affect the production of carbon soot and fullerenes. The *J*x*B* force tends to reduce the effect of gravity when B_0 is sufficiently large. The type A and the Type E are less suitable for the production of fullerenes.

3.3. Production of SWNTs

The production of high-quality SWNTs is one of the most important targets in advancing nanomaterial development. The growth model of SWNTs in the arc-discharge reactors has not been confirmed. Several models show importance of catalyst particles in the hot gas, carbon density and catalyst temperature. [14, 15] Here, the production of SWNTs is examined using the *J*x*B* arc-jet method, which could modify the growth reactions in the hot gas. In this case, a Ni/Y catalyst is included in the carbon material rods (6.0 x 6.0 mm, rectangular type, 4.2 W% of Ni and 0.9 W% of Y included), and *p*(He)= 60 kPa and I_d= 50 A. The soot production rate as a function of applied magnetic field is shown in Fig. 9(a) [16, 17]. By increasing the magnetic field, the production rate monotonically increases. However, further increasing B_0 to above 3.5 mT makes the discharge unstable. Figure 9(b) shows the pressure dependence of the soot production rate for B_0= 0 and B_0= 2.2 mT. As the pressure increases and the collisional effect of He gas increases, the *J*x*B* force clearly affects soot production.

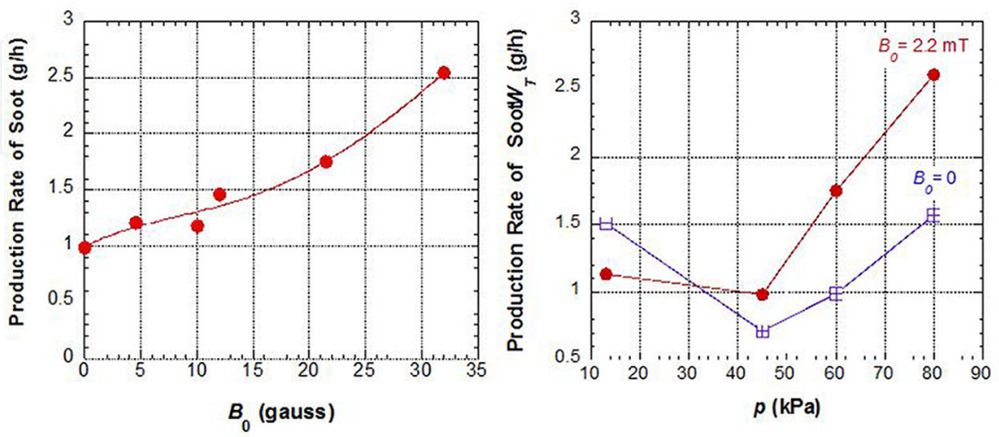

Figure 9. Production rate of soot including SWNTs versus B_0 (a), where *p*(He)= 60 kPa and I_d= 50 A, and pressure dependence (b), where I_d = 50 A.

Using this *J*x*B* arc-jet method, a large amount of SWNTs is produced from carbon rods including a Ni/Y catalyst. Figure 10 shows a typical TEM image of the produced soot, in which many bundles of SWNTs are included. There are also carbon nanoparticles and catalyst nanoparticles in the soot, which should be removed during the purification of the SWNT products. The quality of the products is measured by a Raman spectrometer (Jasco Co., NR-1800. An Ar ion laser of λ= 488.0 nm is used.), and the results are shown in Figs. 11 (a) and 11(b) for B_0= 0 and B_0= 3.2 mT. In both cases, there are very small D(disorder) band peaks and large G (graphite) band peaks, from which we can estimate the content and quality of SWNTs in the produced carbon soot. These figures show that the *J*x*B* arc discharge does not degrade the quality of the SWNTs. From the signals of the radial breathing mode in Fig. 11(a), we can evaluate the SWNT diameters [18]. The major diameter is 1.40 nm, and SWNTs with a diameter of 1.26 nm also exist in the case of B_0= 3.2 mT. SWNTs with diameters of 1.70 nm, 1.16 nm and 1.0 nm also exist in the case of B_0= 0.

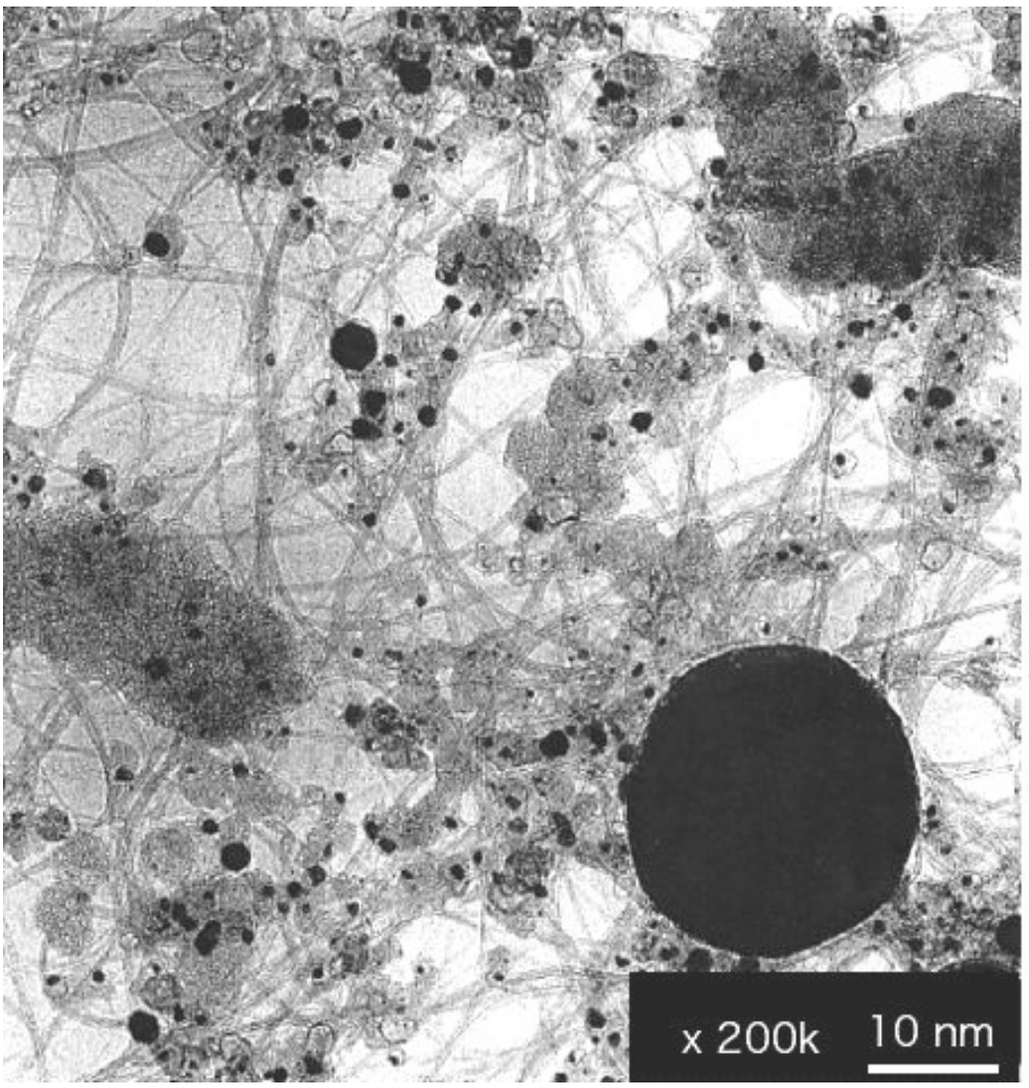

Figure 10. Typical TEM image of SWNTs produced by the *J*x*B* arc-jet discharge method.

http://dx.doi.org/10.5772/51964

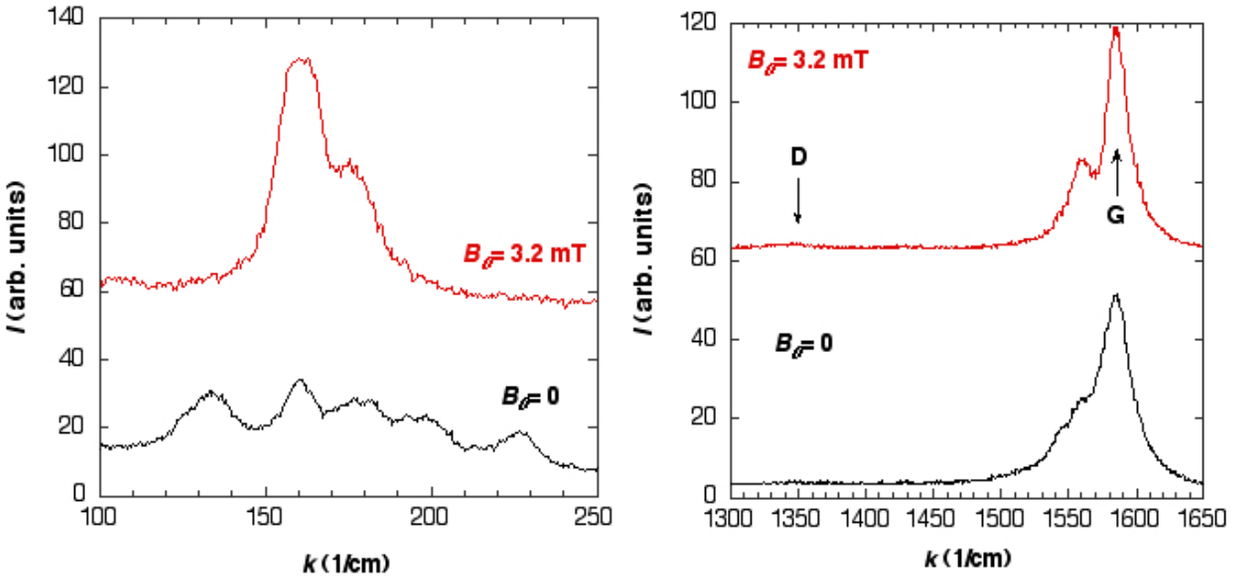

Figure 11. Raman spectra of the produced samples for magnetic fields of B_0= 3.2 mT and 0 T. p(He)= 60 kPa and I_d= 50 A. λ = 488.0 nm.

Figure 12. Photograph of SWNTs dispersed in pure water.

In the arc production of SWNTs, effect of gas species is examined. Ar, Ne or N_2 gas is used instead of He gas, all of which degrade production of SWNTs. When amount of H_2 gas is included in He gas, the SWNT production rate considerably decreases, which is not consistent with the previous report [19]. It is conjectured that He atom has high ionization potential, and it causes almost no chemical reactions and less emission loss. When Co or Fe particles are used as catalyst material instead of Ni/Y particles, the SWNT production rate considerably decreases. However, in case of of Co catalyst, a little amount of very long bundles of SWNTs is obtained, which is about 5 cm long. Improvement of the long-SWNT yield by this method is one of our study targets.

Usually SWNTs have poor dispersibility in water, which limits their potential applications. Therefore, the development of water-dispersible SWNTs is very important. Here we attempt to dissolve a SWNT sample in pure water. First, a small amount of SWNTs is placed in 20 mL of pure water, which is then mixed using a supersonic homogenizer (Sonics Co., VC-130, 25 W) for about 40 min. Then, a small amount of surfactant is added, which is one of biopolymers [20, 21]. And it is mixed by sonication again for about 40 min. As a result, the SWNTs are well dispersed in water, and the dispersion remains very stable for more than 1 month. Figure 12 shows a photograph of SWNTs dispersed in water after 50 times dilution. The study of SWNTs dispersed in water is continuing with the aim of realizing biological applications.

3.4. Production of endohedral metallofullerenes

Using the above arc-jet discharge methods, endohedral metallofullerenes (such as Gd@C_{82} and La@C_{82}) [22] and carbon nanocapsules are efficiently produced. Applications of these materials are expected.

By performing arc discharge using a Gd_2O_3-containing carbon rod (6.0 x 6.0 mm, rectangular), metallofullerenes are produced, where p(He)= 50 kPa and I_d= 58 A. The production rate of soot is about 2.5 g/h. Figure 13(a) shows a typical TEM image of the sample obtained, in which gadolinium nanoparticles with a diameter on the order of 10 nm are covered with carbon atoms, resulting in the formation of carbon capsules with a size of 10 – 50 nm, which are very stable in air. By refluxing the sample with toluene, fullerenes can be extracted from the soot. After 4 h of reflux, the liquid is filtered and a reddish liquid is obtained. A mass spectrum of this sample obtained using a laser-desorption time-of-flight mass spectrometer (LD-TOF-MS) (Bruker Co., Autoflex, + ion mode, 50 shots averaged) is shown in Fig. 13(b). We can confirm the existence of not only C_{60} and higher fullerenes but also endohedral metallofullerenes Gd@C_{82}. Although the peak intensities are not quantitative, the relative yield of Gd@C_{82} compared with that of C_{60} is several mol%. The Gd@C_{82} is expected to be used as a contrast agent in MRI [23].

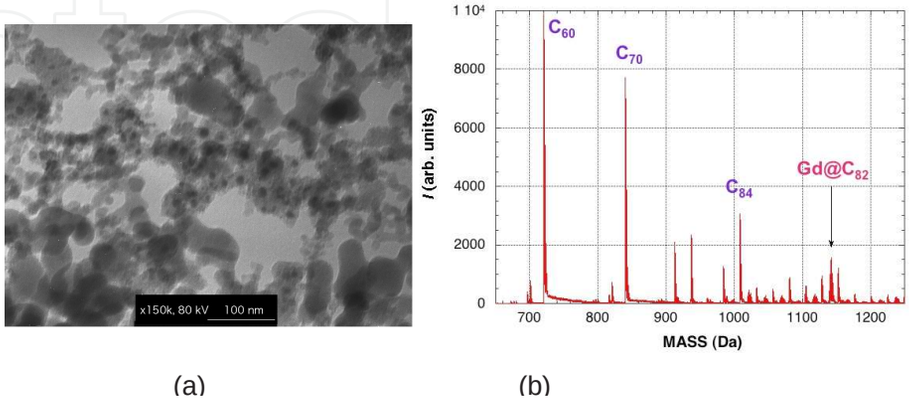

Figure 13. (a) TEM image of gadolinium-continuing carbon nanoparticles produced by the arc-jet discharge method. (b) LD-TOF-MS spectrum of a carbon sample extracted from soot using toluene.

http://dx.doi.org/10.5772/51964

3.5. Production of magnetic nanoparticles

Using the *JxB* arc-jet discharge method, many types of metal-particle-encapsulated carbon nanoparticles [24, 25] can be easily produced. As examples, iron-encapsulated carbon nanoparticles and cobalt-encapsulated carbon nanoparticles have been produced. Both are ferromagnetic nanoparticles with a size of 10 - 100 nm, and are very stable.

Using iron-containing carbon rods (6.0 x 6.0 mm, rectangular), iron-encapsulated carbon nanoparticles are produced, where p(He)= 50 kPa and I_d= 50 A. The soot production rate is about 0.43 g/h. Figure 14 (a) shows a photograph of the produced soot suspended by a magnet, demonstrating the good ferromagnetic property. A typical TEM image of the sample is shown in Fig. 14 (b). Iron particles with a size of 1 nm to 20 nm are covered with carbon atoms, resulting in the formation of carbon particles with a size of 10 – 100 nm. These particles are very stable in air and inactive in hydrochloric acid.

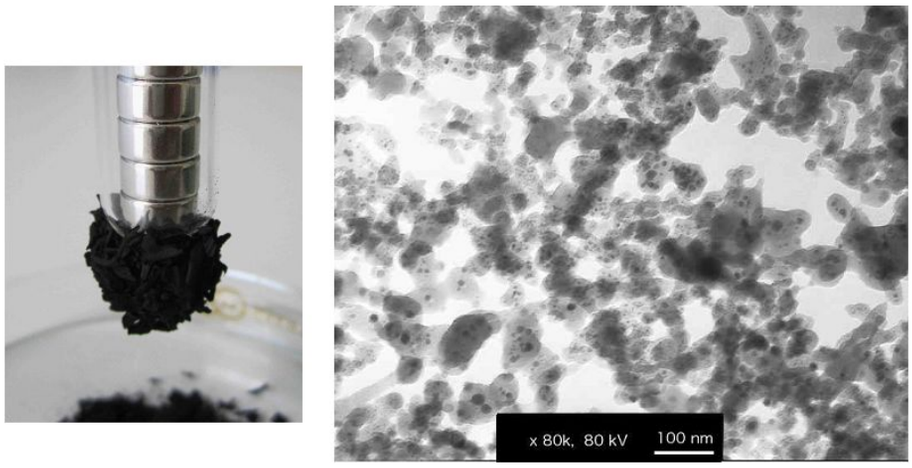

Figure 14. (a) Photograph of iron-containing carbon nanoparticles suspended by a magnet. (b) TEM image of iron-containing carbon nanoparticles.

Figure 15. Photograph of iron-containing carbon nanoparticles dispersed in water.

Cobalt-encapsulated carbon nanoparticles, which also have ferromagnetic properties, are produced by the arc-jet discharge method. They are dispersed in pure water with a small amount of surfactant (gelatin *etc*.) and mixed using a supersonic homogenizer (Sonic Co., VX-130) for 1 h. Finally, a black inklike liquid is obtained. The dispersion is homogeneous and stable, and most of the particles do not precipitate even after one month. These water-soluble magnetic nanoparticles potentially have many applications in the fields of liquid sealing, medical diagnostics and medical treatment [26]. Figure 15 shows a photograph of the stable iron-containing carbon nanoparticles dispersed in water.

4. Development of automatic *JxB* arc-jet producer

To produce SWNTs and carbon nanoclusters at a commercial scale by the *JxB* arc-jet discharge method, a revolver-injection-type arc jet producer (RIT-AJP) has been developed by collaboration with Daiavac Ltd. (Japan) [9].

A schematic and photograph of RIT-AJP are shown in Fig. 16. The left side of the machine is an arc discharge chamber, which consists of a vacuum vessel made of stainless steel 25 cm in diameter and 70 cm high that is uniformly cooled by water jackets. About 5 L of water is stored in the jackets and cooling water is slowly supplied to the jackets. In the central part of the chamber, a cathode electrode (30 mm in diameter), an anode electrode, an exhaust port, a viewing port and an electrode-cleaning hand are mounted. The top and bottom parts of the chamber are soot collectors, with an inner diameter of about 25 cm and a height of 24 cm, in which produced soot is deposited. Using these collectors, as much as 25 L of soot can be easily collected after a single operation.

The right side of the apparatus is a revolver-type carbon rod magazine. In the cylindrical metal vacuum vessel, which is 34 cm in diameter and 49 cm long, there is a rotatable cylindrical magazine, in which as many as 50 carbon rods of 6 - 10 mm diameter and 300 mm length can be loaded. A schematic figure of the material-feeding mechanism of the magazine is shown in Fig. 17(a), and a photograph of a rotatable carbon rod magazine (for 50 carbon rods) is shown in Fig. 17(b). Under the vacuum chamber, there is a vacuum pump, an electrical controller and a microcomputer. Discharge power is supplied by an inverter-type DC power supply (Daihen Co., ARGO-300P).

The production sequence is as follows. First, up to 50 carbon rods are loaded in the magazine, and the chamber is evacuated by the vacuum pump. After evacuation to a pressure of less than 10 Pa, pure helium gas is introduced and the chamber is closed. Upon turning on the electrical controller, a metal striker pushes one of the carbon rods towards the cathode, and the discharge starts upon electrical contact. As the discharge conditions are determined by the discharge voltage and discharge current, the carbon rod is automatically moved until both parameters match the set values. Once the carbon rod is consumed, the cylindrical carbon magazine rotates 1/50 of a turn and the next carbon rod is inserted by the striker. A magnetic field can be applied by a block-type ferrite magnet located outside the chamber, by which a magnetic field of about 2 mT is applied horizontally to the discharge space. Carbon

http://dx.doi.org/10.5772/51964

deposited on the cathode is removed by a cathode-cleaning hand. After the discharge, produced soot that has been deposited is carefully collected.

As an example of the continuous production of carbon clusters, fullerenes are produced. Using 134 carbon rods of 8 mm diameter, continuous *J*x*B* arc-jet discharge is carried out, where p(He)= 40 kPa, the discharge current is I_d= 120 A, the voltage between electrodes is V_{rod}~ 33 V and the gap distance is d_G~ 5 mm. The insertion speed of the carbon rods is about 30 cm/h. After the discharge, carbon soot from three parts (the top collector, central chamber and bottom collector) is collected separately and their masses are measured. The amount of soot deposited on the top wall is considerably increased by applying the magnetic field, because the carbon molecules are blown upward onto the top wall. After sufficient mixing, the C_{60} content in the soot is measured by a UV/visible spectrometer (Shimadzu Co. UV-1200). At the top collector, the C_{60} content is the highest and about 14 W% of C_{60} is present, whereas, 4.2 W% is present on the center wall and 2.9 W% is present on the bottom wall. In total, about 105 g of soot containing about 7 g of C_{60} is produced in 12 h.

The contents of higher fullerenes in the soot are measured using a high-pressure liquid chromatograph (HPLC) (Jasco Co., Gulliver Series, PU980) [27]. The collection rates of C_{60}, C_{70}, C_{76}, C_{78} and C_{84} for two different magnetic fields are shown in Fig. 18. White rectangules in the graphs show the measurement errors. By applying a magnetic field, the collection rates of these fullerenes considerably increase.

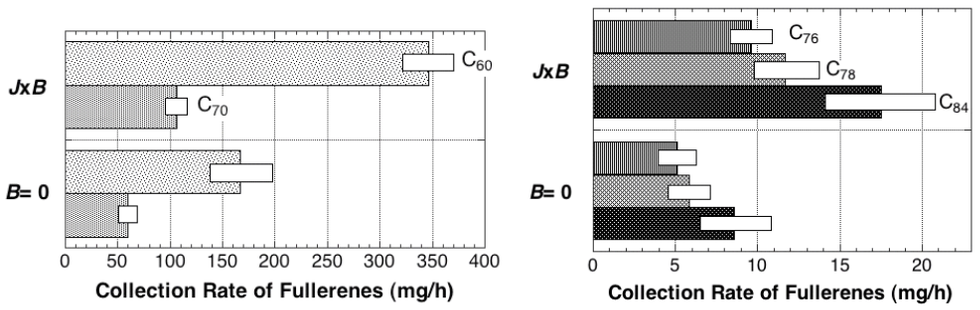

Figure 18. Collection rates of C_{60} and C_{70} (a), and C_{76}, C_{78} and C_{84} (b) for two different magnetic fields.

5. Summary

1. By applying a steady state magnetic field perpendicular to the discharge current, *J*x*B* arc-jet discharge is successfully produced. The flow of hot gas and the heat flux are concentrated in the *J*x*B* direction.
2. Carbon atoms sublimated from the anode are continuously ejected from the arc plasma in the *J*x*B* direction. As a result of the *J*x*B* force, the effect of gravity (heat convection) can be reduced.

3. By increasing the magnetic field, the production rate of carbon soot including SWNTs considerably increases, in which the quality of the SWNTs remains high. Water-soluble SWNTs can be obtained by additional processing.

4. Using the *J*x*B* arc-jet discharge, endohedral metallofullerenes, Gd@C_{82} and magnetic nano-particles (iron-encapsulateted carbon nanoparticles and cobalt-encapsulated carbon nano-particles) are sucessfully produced.

5. For the continuous and large-scale production of carbon clusters, a revolver-injection-type arc-jet producer (RIT-AJP) has been developed. Using this machine, the automatic mass production of SWNTs and carbon clusters is realized. We are currently attempting to fabricate many new types of carbon clusters using this machine.

Acknowledgments

We thank H. Inoue of Daiavac Co. (Chiba, Japan) for his technical support during the development of the RIT-AJP machine. We also thank W. Tomoda, Md. K. H. Bhuiyan and S. Aoyama of Shizuoka University for their technical assistance.

Author details

Tetsu Mieno and Naoki Matsumoto

Department of Physics, Shizuoka University, Japan

References

[1] Iijima, S. Single-Shell Carbon Nanotubes of 1-nm Diameter, Nature 1993; 363, 603-605.

[2] Bethune, D. S., Klang, M. S., de Vries, M. S., Gorman, G., Savoy, R., Vazquez, J., Beyers, R., Cobalt-catalysed growth of carbon nanotubes with single-atomic-layer walls, Nature 1993; 363, 605-607.

[3] Dresselhaus, M. S., Dresselhaus, G., Avouris, Ph., (eds.) Carbon Nanotubes, Springer, Berlin, 2000, ISBN: 3-540-41086-4.

[4] Jorio. A., Dresselhaus, M. S., Dresselhaus, G., (eds.) Carbon Nanotubes, Springer, Berlin, 2008, ISBN : 978-3-540-72864-1.

[5] Harris, P. J. Carbon Nanotubes Science, Cambridge University Press, Cambridge, 2009, ISBN: 978-0-521-53585-4.

[6] Journet, C., Maser, W. K., Bernier, P., Loiseau, A. Lamy de la Chapele, M., Lefrant, S., Deniard, P., Lee, R., Fischer, J. E., Large-scale production of single-walled carbon nanotubes by the electric-arc technique, Nature, 388, pp. 756-758.

[7] Mansour, A., Razafinimanana, M., Monthoux, M., Pachco, M., Gleizes, A., A siginificant improvement of both yield and purity during SWNT synthesis via the electric arc process, Carbon, 45, 2007, pp. 1651-1661.

[8] Mieno, T. Automatic Production of Fullerenes by a *JxB* Arc Jet Discharge Preventing Carbon Vapor from Depositing on the Cathode, Fullerene Science & Technology 1995; 3 (4), 429-435.

[9] Mieno, T. *JxB* Arc Jet Fullerene Producer with a Revolver Type Automatic Material Injector, Fullerene Science & Technology 1996; 4 (5), 913-923.

[10] Mieno, T. Production of Fullerenes from Plant Materials and Used Carbon Materials by Means of a Chip-Injection-Type *JxB* Arc Reactor, Fullerene Science & Technology 2000; 8 (3), 179-186.

[11] Matsumoto, N., Mieno, T. Characteristics of Heat Flux of *JxB* Gas-Arc Discharge for the Production of Fullerenes, Vacuum 2003; 69, 557-562.

[12] Jahn, R. G. Physics of Electric Propulsion, McGraw-hill, New York, 1968, 257-316, (NC)ID: BA18312459.

[13] Aoyama, S., Mieno, T. Effects of Gravity and Magnetic Field in Production of C_{60} by a DC Arc Discharge, Japanese Journal of Applied Physics 1999; 38 (3A), L267- L269.

[14] Kanzow, H., Ding, A, Formation mechanism of single-wall carbon nanotubes on liquid-metal particles, Physical Review B 1999 ; 60 (15) 11180-11186.

[15] Gavillet, J. *et al.*, Microscopic mechanisms for the catalyst assisted growth of single-wall carbon nanotubes, Carbon 2002 ; 40, 1649-1663.

[16] Mieno, T., Tan, G.-D. Effect of Gravity and Magnetic Field on Production of Single-Walled Carbon Nanotubes by Arc-Discharge Method, In: Yellampalli, S. (ed.) Carbon Nanotubes- Synthesis, Characterization, Application; InTech; 2011, 61-76, ISBN: 978-953-307-497-9.

[17] Mieno, T., Matsumoto N., Takeguchi, M. Efficient Production of Single-Walled Carbon Nanotubes by *JxB* Gas-Arc method, Japanese Journal of Applied Physics 2006; 43 (12A), L1527- L1529.

[18] Kataura, H. *et al.* Optical Properties of Single-Walled Carbon Nanotubes, Synthetic Metals 1999; 103, 2555-2558.

[19] Zhao, X., Inoue, S., Jinno, M., Suzuki T., Ando Y., Macroscopic oriented web of single-wall carbon nanotubes, Chemical Physics Letters 2003; 373, 266-271.

[20] Takahashi, T., Tsunoda, K., Yajima, H., Ishii, T., Purification of Single Wall Carbon Nanotubes Using Gelatin, Japanese Journal of Applied Physics 2004; 43 (3), 1227-1230.

[21] Takahashi, T., Luculescu, C. R., Uchida, K., Tsunoda, K., Yajima, H., Ishii, T., Dispersion Behavior and Spectroscopic Properties of Single-Walled Carbon Nanotubes in Chitosan Acidic Aqueous Solutions, Chemistry Letters 2005; 34 (11), 1516-1517.

[22] Shinohara, H., Endohedral metallofullerenes, Reports on Progress in Physics 2000; 63, 843-892.

[23] Mikawa, M. *et al.* Paramagnetic Water-Soluble Metallofullerenes Having the Highest Relaxivity for MRI Contrast Agents, Bioconjugate Chemistry 2001; 377, 510-514.

[24] Saito, Y., Nanoparticles and Filled Nanocapsules, Carbon 1995; 33 (7) 979-988.

[25] Saito, Y. *et al.* Iron particles nesting in carbon cages grown by arc discharge, Chemical Physics Letters 1993; 212 (3-4) 379-383.

[26] Pankhurst, Q. A., Connolly, J., Jones, S. K., Dobson, J. Applications of Magnetic Nanoparticles in Biomedicine 2003; 36, R167-R181.

[27] Bhuiyan, Md. K. H., Mieno, T. Production Characteristics of Fullerenes by Means of the *JxB* Arc Discharge Method, Japanese Journal of Applied Physics 2002; 41 (1), 314-318.